Electrocardiographic assessment of repolarization heterogeneity

Hooft van Huysduynen, Bart

Chapter 7

Dispersion of the repolarization in cardiac resynchronization therapy

Bart Hooft van Huysduynen
Cees A. Swenne
Jeroen J. Bax
Gabe B. Bleeker
Harmen H.M. Draisma
Lieselot van Erven
Sander G. Molhoek
Hedde van de Vooren
Ernst E. van der Wall
Martin J. Schalij

Heart Rhythm 2005; 2: 1286-93

ABSTRACT

Background. Pro-arrhythmic effects of cardiac resynchronization therapy (CRT) have been described in a subset of vulnerable patients as a result of increased transmural dispersion of repolarization (TDR) induced by left ventricular (LV) epicardial pacing. The possibility of identifying these patients by repolarization indices on the electrocardiogram has been suggested. The purpose of this study was to test whether repolarization indices on the ECG can be used to measure dispersion of the repolarization during pacing.

Methods. CRT devices of 28 heart failure patients were switched among BIV, LV and right ventricular (RV) pacing. Electrocardiographic indices proposed to measure dispersion of the repolarization were calculated. The effects of CRT on repolarization were simulated in ECGSIM, a mathematical model of electrocardiogram genesis. TDR was calculated as the difference in repolarization time between the epi- and endocardial nodes of the heart model.

Results. *Patients.* The interval from the apex to the end of the T wave was shorter during BIV pacing (102 ± 18 ms) and LV pacing (106 ± 21 ms) than during RV pacing (117 ± 22 ms, $P \leq 0.005$). T-wave amplitude and area were low during BIV pacing (287 ± 125 μV and 56 ± 22 μV·s, respectively, $P = 0.0006$ vs. RV pacing), T-wave complexity was high during BIV pacing (0.42 ± 0.26, $P = 0.004$ vs. RV pacing). *Simulations.* Repolarization patterns were highly similar to the preceding depolarization patterns. The repolarization patterns of different pacing modes explained the observed magnitudes of the electrocardiographic repolarization indices. Average and local TDR were not different between pacing modes.

Conclusions. In patients treated with CRT, electrocardiographic repolarization indices are related to the pacing-induced activation sequences rather than to transmural dispersion. TDR during BIV and LV pacing is not larger than during conventional RV endocardial pacing.

INTRODUCTION

Cardiac resynchronization therapy (CRT) restores coordinated mechanical contraction in most heart failure patients with compromised intraventricular conduction[1;2]. Application of CRT reduces the occurrence of heart failure[3] and all cause mortality[4]. However, CRT may have pro-arrhythmic effects in a subset of vulnerable patients due to increased dispersion of the repolarization[5;6]. Left ventricular epicardial pacing reverses the natural activation from endo- to epicardium. This advances the repolarization time of the already short epicardial action potentials, thereby increasing repolarization time differences with the longer underlying action potentials of the midmyocardial and endocardial layers. The thus increased transmural dispersion of repolarization (TDR) may enhance the susceptibility to arrhythmias. It would be of great clinical value if vulnerable patients could be identified by a noninvasive repolarization measure on the electrocardiogram (ECG) such as the interval from the apex to the end of the T wave (Tapex-end) [7].

The Tapex-end interval as a measure of dispersion of the repolarization was proposed on the basis of experiments in a wedge preparation of the left ventricular wall[8]. Although being a valuable research tool, the wedge preparation represents only part of the heart and the pseudo-ECG derived from this preparation is probably not representative for clinical ECGs. Other proposed ECG indices of dispersion of the repolarization are also difficult to verify in vivo, as in most studies either epi- or endocardial repolarization is recorded from a limited number of electrodes on the heart[9;10].

In the current study we used a whole heart model of ECG simulation, ECGSIM[11] to study whether epicardial pacing in CRT increases TDR. Moreover, we sought to clarify how the repolarization process during CRT is reflected in ECG indices proposed to measure dispersion of the repolarization.

METHODS

Patients

Twenty-eight heart failure patients were studied two days after implantation of a biventricular pacemaker at the Leiden University Medical Center. The characteristics of these patients are listed in *Table 1*. After the patients had rested supine for five minutes, standard 12-lead ECGs were recorded continuously while the pacemaker was programmed in random order in biventricular (BIV), left ventricular (LV), and right ventricular (RV) mode, and turned off, for three minutes per mode. The last minute of these ECG recordings was subsequently analyzed.

ECG characteristics	SR	RV pacing	LV pacing	BIV pacing
Heart rate (bpm)	73 ± 11	72 ± 14	72 ± 12	73 ± 11
QRS duration (ms)	175 ± 31	191 ± 31	167 ± 36	146 ± 17
QTc (ms)	503 ± 47	512 ± 45	487 ± 31	477 ± 44
Tapex-end$_c$ (ms)	108 ± 27	117 ± 22	106 ± 21	102 ± 18
Tamplitude (μV)	362 ± 219	478 ± 174	335 ± 143	287 ± 125
Tarea (μV.s)	66 ± 31	94 ± 35	62 ± 26	56 ± 22
Tcomplexity (.)	0.30 ± 0.13	0.25 ± 0.10	0.36 ± 0.19	0.42 ± 0.26
QRS-T angle (°)	162 ± 20	167 ± 9	149 ± 28	154 ± 21

Table 1. *Patient characteristics.*

ECG analysis was performed by LEADS (Leiden ECG Analysis and Decomposition Software), our MATLAB (The MathWorks, Natick, USA) program for research oriented ECG analysis. LEADS first computed an averaged beat in order to minimize noise. In this averaged beat, the beginning and end of the QRS complex were automatically detected. An observer, who was blinded to the patient data, corrected this interval if necessary. LEADS identified the apex and end of the T wave in each ECG lead. The end of the T wave was set at the point where the tangent to the steepest portion of the terminal part of the T wave crossed the isoelectric line. Subsequently, LEADS searched backward for the apex of the T wave, defined as the

point of the T wave with the highest amplitude. Finally, LEADS calculated a number of ECG indices proposed to assess dispersion of the repolarization: the Tapex-end interval[8], QT interval[12], T-wave amplitude[13], T-wave surface area[14] and T-wave complexity[15]. QT and Tapex-end intervals were corrected for heart rate by the Bazett formula[16]. T-wave complexity was calculated by means of singular value decomposition of the T wave[15;17]. The higher, more complex, singular values 2 to 8 were divided by the first, most simple component to quantify T-wave complexity. Additionally, LEADS constructed the vectorcardiogram by using the inverse Dower matrix[18;19] and calculated the spatial angle between the QRS and T axes.

Simulations

ECGSIM is an ECG simulation program that consists of a mathematical whole heart model placed in a human thorax[11]. The model geometry is based on magnetic resonance images of heart and thorax, containing conduction inhomogeneities such as the lungs. Surfaces of the left and right ventricle consist of 257 epicardial and endocardial nodes. A transmembrane action potential in each node represents the local electrical activity[13]. The naturally present TDR is incorporated in the model: the epicardium has shorter action potential durations than the endocardium, so that despite earlier endocardial activation the epicardium repolarizes earlier. The specific electrophysiological properties of all 257 nodes can be found after downloading the model from www.ecgsim.com (free of charge). With default parameter settings, ECGSIM generates an ECG that closely resembles the ECG of a healthy subject.

For the current study, the activation sequences associated with pacing were based on previously published depolarization maps[20-24]. A left posterolateral node, node #79, was chosen as the location of the LV epicardial pacing site. The averaged QRS duration measured in the heart failure patients was adopted as the total time of ventricular depolarization. The moment of activation of each node was calculated by multiplying the total time of depolarization by the ratio of the distance of each node from the pacing site to the total distance the activation front needed to travel to activate the entire heart. The action potential durations of all nodes were left unaltered. The repolarization times of all nodes were calculated by addition of the action potential durations to the moments of activation.

RV pacing was simulated likewise. The heart was activated from a RV apical endo-

cardial node, node #249. BIV pacing was simulated by simultaneous pacing from nodes ## 79 and 249, thus combining the ventricular depolarization and repolarization times of LV and RV pacing. Thereafter, ECGSIM constructed isochrone maps of depolarization and repolarization times of the heart. The simulated ECGs were analyzed with the LEADS program as described above.

For comparison with normal ventricular activation with an intact conduction system, we used the default settings of de- and repolarization times of ECGSIM, which generates a normal ECG.

Subsequently, we calculated TDR for the different pacing modes and during normal activation. Each endocardial node was paired with an opposing epicardial node, and TDR was calculated as the difference in repolarization time between the endo- and epicardial node[25]. As there are more epicardial than endocardial nodes, several endocardial nodes had two opposing epicardial nodes. In these cases, the difference was calculated between the repolarization time of the endocardial node and the mean repolarization time of the two opposing epicardial nodes. Similarly, each LV septal node was paired with one or two RV septal nodes. Subsequently, all paired repolarization time differences were averaged to calculate TDR. Additionally, we measured local TDR directly under the LV epicardial pacing site during LV pacing and during normal ventricular activation. Similarly, local TDR in the septum directly under the RV endocardial pacing site was calculated.

Statistical Analysis

Repeated measures ANOVA was performed before post-hoc t-testing. Two-sided paired t tests were used to compare data between different pacing modes. *P*-values were Bonferroni corrected for multiple testing. A probability value of $P < 0.05$ was considered significant.

RESULTS

Patients

Four ECGs recorded during sinus rhythm, RV pacing, LV pacing and BIV pacing are depicted in *Figure 1, panels A-D*. All ECGs were highly discordant: QRS- and T-wave polarities were opposite in almost all leads of every rhythm. Consequently, as shown in Table 2a, the spatial angles between the QRS and T axes (a gross qualifier of concordance / discordance) were close to 180°. The largest average spatial QRS-T angle was attained during RV pacing. Correlation coefficients of the spatial orientation of the QRS- and T-vectors were 0.96 for RV pacing, 0.79 for LV pacing and 0.85 for BIV pacing.

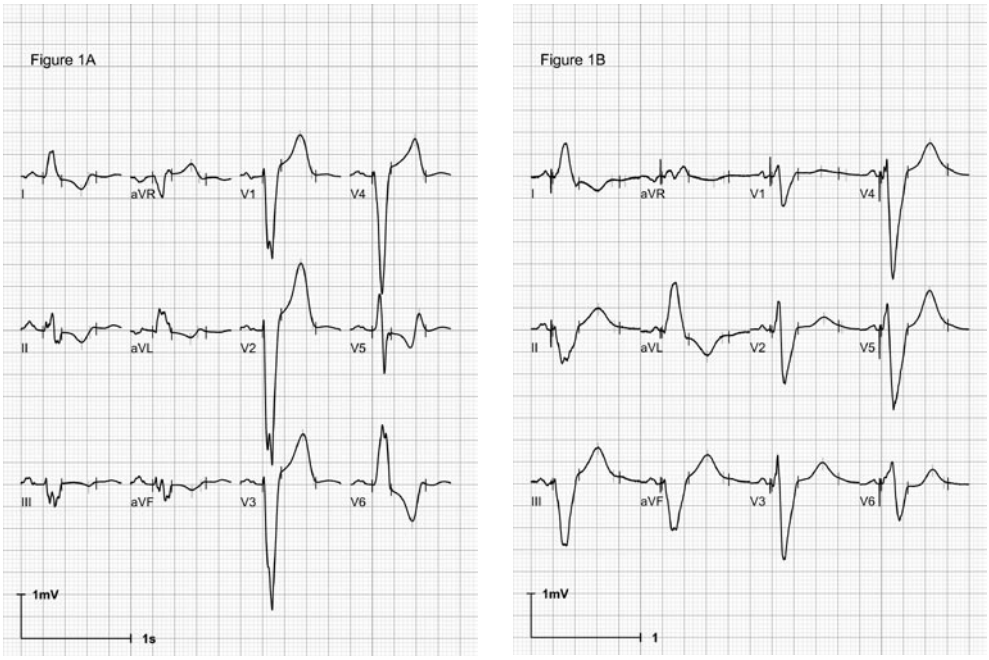

Figure 1. *Sample ECGs (average beat) during sinus rhythm, right-, left-, and biventricular pacing. Panel A. Subject #08 in sinus rhythm,Panel B. Subject #26 during right ventricular pacing*

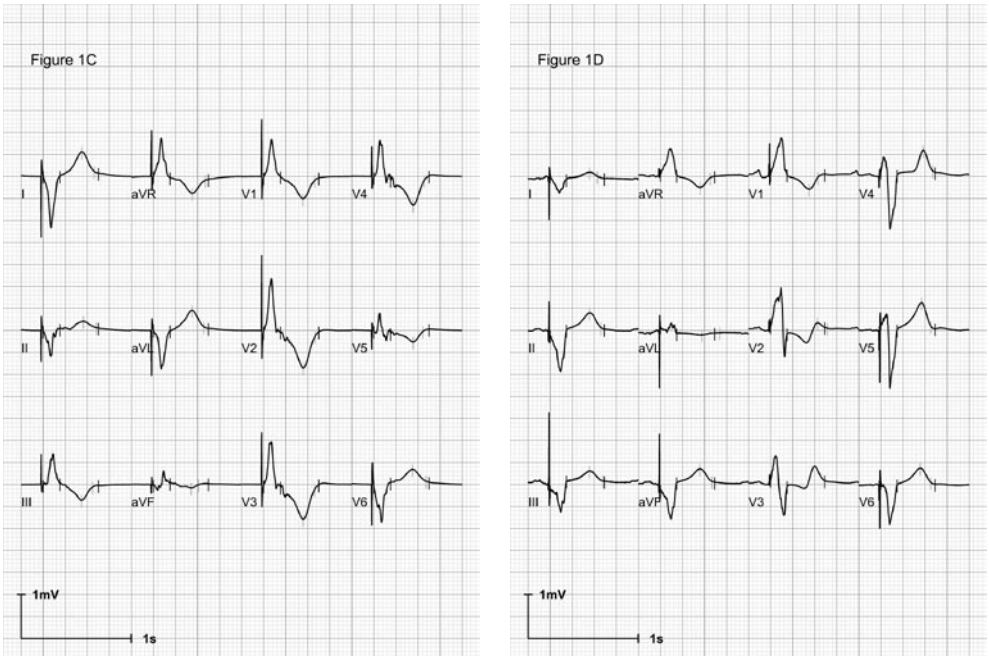

Figure 1. *Sample ECGs (average beat) during sinus rhythm, right-, left-, and biventricular pacing. Panel C. Subject #19 during left ventricular pacing Panel D. Subject #07 during biventricular pacing.*

ECG characteristics	SR	RV pacing	LV pacing	BIV pacing
Heart rate (bpm)	73 ± 11	72 ± 14	72 ± 12	73 ± 11
QRS duration (ms)	175 ± 31	191 ± 31	167 ± 36	146 ± 17
QTc (ms)	503 ± 47	512 ± 45	487 ± 31	477 ± 44
Tapex-end$_c$ (ms)	108 ± 27	117 ± 22	106 ± 21	102 ± 18
Tamplitude (μV)	362 ± 219	478 ± 174	335 ± 143	287 ± 125
Tarea (μV.s)	66 ± 31	94 ± 35	62 ± 26	56 ± 22
Tcomplexity (.)	0.30 ± 0.13	0.25 ± 0.10	0.36 ± 0.19	0.42 ± 0.26
QRS-T angle (°)	162 ± 20	167 ± 9	149 ± 28	154 ± 21

Table 2a. *ECG characteristics of heart failure patients during different rhythms. Data are given in average ± standard deviation. SR = sinus rhythm; RV = right ventricular; LV = left ventricular; BIV = biventricular.*

ECG characteristics	RV vs LV pacing	LV vs BIV pacing	BIV vs RV pacing
Heart rate (bpm)	1	1	1
QRS duration (ms)	0.002	0.004	< 0.0001
QTc (ms)	0.005	1	0.003
Tapex-end$_c$ (ms)	0.0009	1	0.005
Tamplitude (μV)	0.0006	0.6	< 0.0001
Tarea (μV.s)	0.0006	1	< 0.0001
Tcomplexity (.)	0.048	1	0.004
QRS-T angle (°)	0.02	1	0.008

Table 2b. *P-values for all ECG differences between different pacing modes. RV = right ventricular; LV = left ventricular; BIV = biventricular.*

Table 2a lists average heart rate, QRS duration and the values of the ECG indices of dispersion of the repolarization. QRS duration was longest during RV pacing and shortest during BIV pacing, LV pacing had intermediate values (see Table 2b for *P*-values). QTc and Tapex-end$_c$ intervals followed the same pattern with decreasing values from RV to LV and BIV pacing. The same applies to T-wave amplitude and area. The pattern present in the above-described ECG indices during different rhythms is depicted in Figure 2. T-wave complexity was large during BIV pacing and small during RV pacing.

Simulations

Depolarization and repolarization maps are depicted in Figure 3. The maps of the normal situation with intact conduction system are shown in panel A, in which de- and repolarization patterns differ significantly. During RV and LV pacing (panels B and C) depolarization spreads from the RV apex and the LV lateral wall, respectively. Here, repolarization roughly follows the depolarization pattern. During BIV pacing (panel D), the heart is activated simultaneously from these two sites. Also here, the repolarization map resembles the depolarization map.

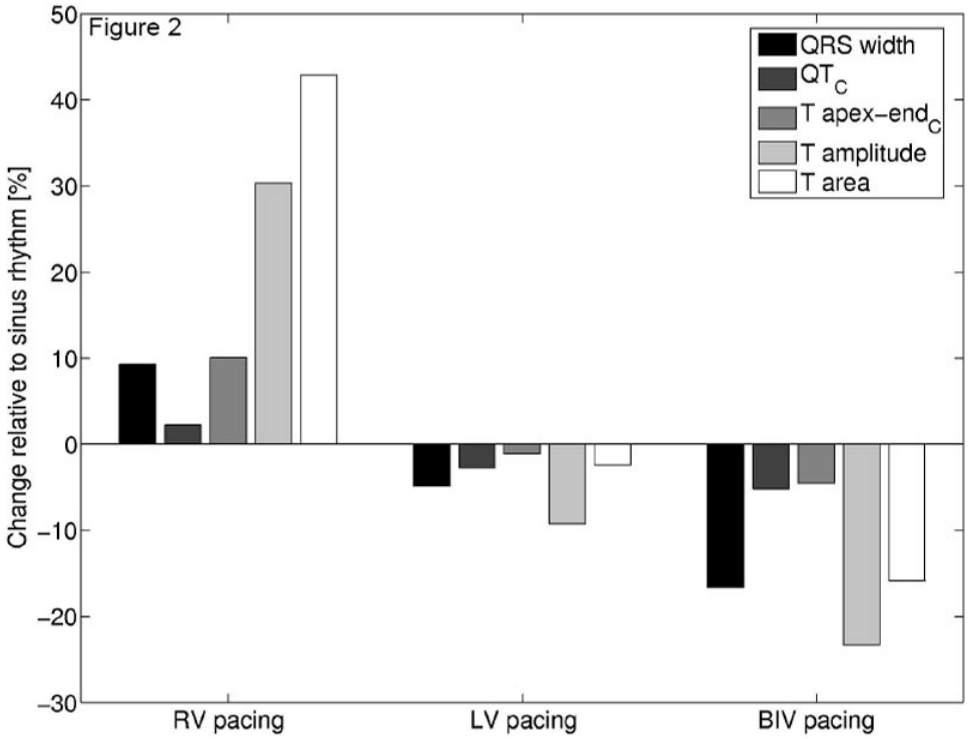

Figure 2. *Values of ECG indices during right ventricular (RV), left ventricular (LV) and biventricular (BIV) pacing relative to sinus rhythm. Values of ECG indices decreased in magnitude from RV-, to LV- to BIV pacing.*

The corresponding simulated ECGs are depicted in Figure 4, panels A-D. During normal ventricular activation (panel A), the ECG is normal, hence highly concordant: the QRS complex and the T wave had a similar polarity in most leads. In all pacing modes the ECGs were highly discordant: the QRS complex and the T wave had opposite polarities in most leads. The spatial angle between the QRS and T axes was small during normal ventricular activation, and close to 180° during pacing.

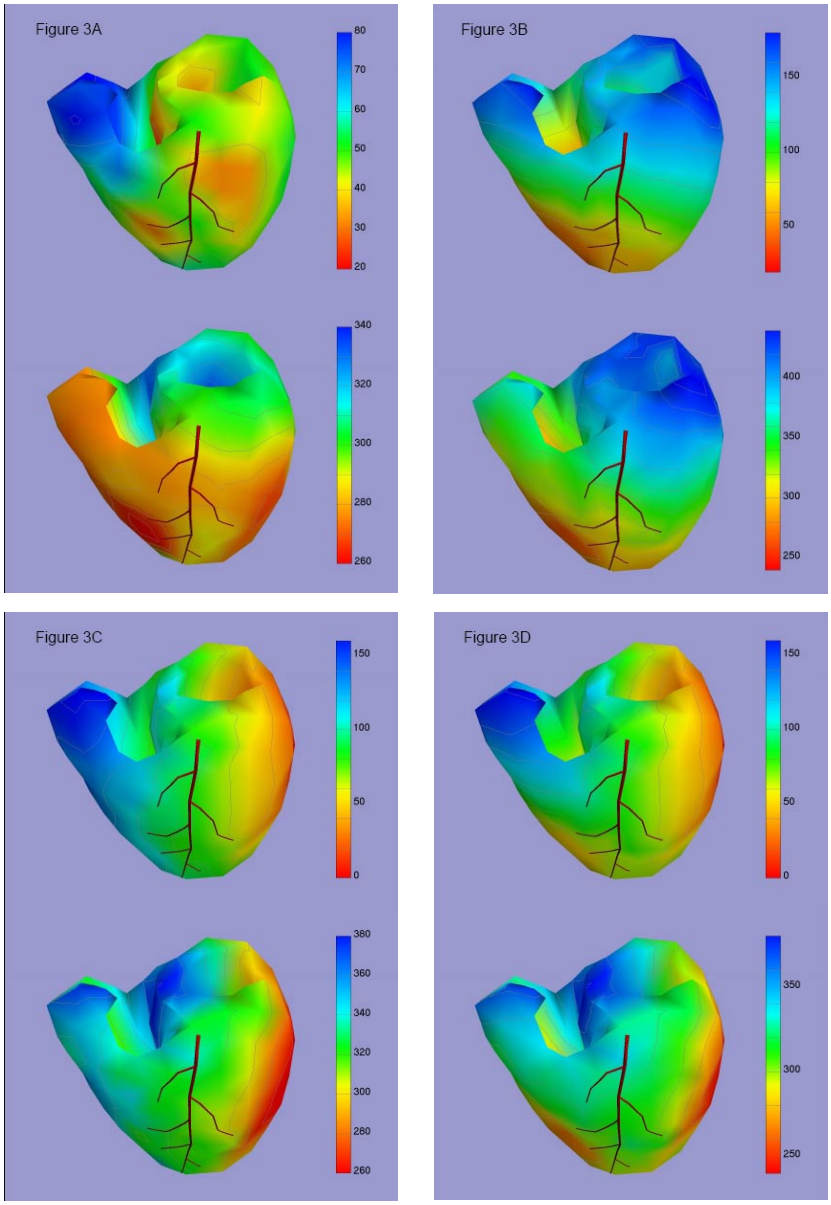

Figure 3. *Simulated depolarization/repolarization maps. Hearts are depicted as viewed from antero-superior with the left anterior descending artery as landmark. Red indicates the earliest depolarization/repolarization and blue indicates the latest depolarization/repolarization. Panel A. Normal ventricular activation, intact conduction system. Panel B. Right ventricular endocardial pacing. Apparently, repolarization patterns are now very similar to depolarization patterns. Panel C. Left ventricular epicardial pacing. Repolarization patterns closely resemble the depolarization pattern. Panel D. Biventricular pacing.*

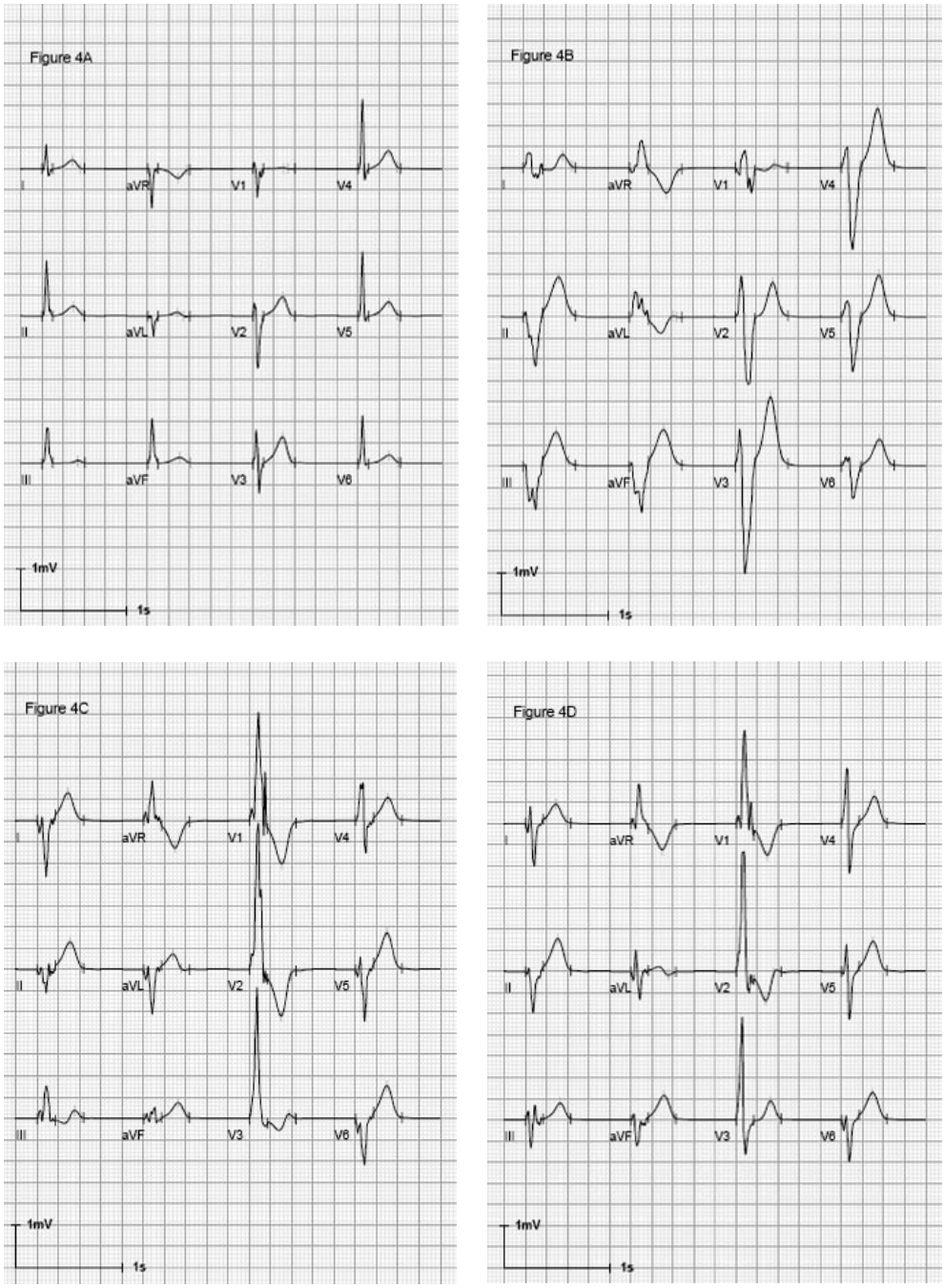

Figure 4. *ECGs generated by ECGSIM. Panel A. Normal ventricular activation, intact conduction system. Panel B. Right ventricular pacing. Panel C. Left ventricular pacing. Panel D. Biventricular pacing*

Table 3 depicts the main characteristics of the simulated ECGs. The values of all ECG repolarization indices were smallest during normal ventricular activation. QRS duration was longest for RV pacing, smaller for LV pacing, while BIV pacing had the smallest paced QRS duration. QTc was longest for RV pacing and smaller during LV and BIV pacing. Tapex-end$_c$ interval was longest for RV pacing, while LV and BIV pacing had a smaller Tapex-end$_c$ interval. T-wave amplitude and area decreased from RV to LV to BIV pacing. T-wave complexity was largest during BIV pacing. QRS-T angle was largest during RV pacing and decreased from LV to BIV pacing; it remained however relatively large.

	normal conduction	**RV pacing**	**LV pacing**	**BIV pacing**
HR (bpm)	60	60	60	60
QRS duration (ms)	100	184	172	166
QTc (ms)	376	450	401	400
Tapex-end$_c$ (ms)	79	104	93	94
Tamplitude (μV)	294	820	679	606
Tarea (μV.s)	36	115	91	80
Tcomplexity (.)	0.13	0.23	0.19	0.36
QRS-T angle (°)	69	168	151	147

Table 3. *ECG characteristics - simulations. RV = right ventricular; LV = left ventricular; BIV = biventricular.*

In ECGSIM, TDR in the whole heart and in the LV free wall was larger during pacing than during normal ventricular activation with intact conduction system, but differences between pacing modes were small. TDR in the whole heart was largest for RV pacing, 29 ms, with slightly smaller values for LV and BIV pacing, 26 and 27 ms respectively, while TDR was 18 ms during normal conduction. TDR in the LV free wall showed the same pattern with slightly higher values; 36 ms for RV pacing, 31 ms for LV pacing and 32 ms for BIV pacing, with a TDR of 19 ms for a normally conducted beat.

Local TDR directly under the LV pacing site increased from 18 ms during normal

ventricular activation to 39 ms during LV epicardial pacing, as a result of the reversal of the naturally existing endo-to epicardial activation order. In the septum directly under the RV pacing site, local TDR increased from 20 to 75 ms during RV endocardial pacing.

DISCUSSION

Our simulations indicate that TDR during LV and BIV pacing was not larger than TDR during conventional RV endocardial pacing, neither in the whole heart nor directly under the pacing sites. In patients treated with CRT, ECG indices of dispersion of the repolarization were measured during different pacing modes. The observed magnitudes of these ECG indices can be explained by interpretation of our simulations.

Principles of repolarization during pacing

In the virtual situation that all myocardial cells would depolarize at the same time instant, only intrinsic differences in action potential duration would determine the repolarization sequence. During normal ventricular activation there is a mix of conduction system mediated rapid depolarization and slower cell-to-cell conduction. In such cases, the repolarization order is partly determined by the order in which the cells depolarize and partly by intrinsic action potential duration differences. In the paced heart, slow cell-to-cell conduction prevails[20-24] and the repolarization order starts to closely resemble the depolarization order; a condition associated with secondary T-wave changes[26].

In our patients as well as in the paced simulations, the QRS complex and the T wave had opposite polarities and the spatial angle between QRS and T axes approximated 180°. Such discordant ECGs emerge when the repolarization sequence roughly equals the depolarization sequence; the opposite polarity is caused by the opposite direction of the repolarizing and depolarizing currents. This view is supported by the simulated ECGs (*Figure 4*) that strikingly resemble the ECGs that were recorded in patients (*Figure 1*). These ECGs could be generated by only changing the ventricular depolarization sequence, while leaving the action potential durations unaffected.

The discordance between the QRS complex and the T wave during pacing are in contrast to the concordance found in the simulated ECGs during normal activation (Figure 4A). During normal activation, the epicardium depolarizes last but repolarizes first due to the relatively short epicardial action potential durations. In combination with the opposite direction of de- and repolarizing currents, a concordant QRS

complex and T wave emerge.

Transmural dispersion of the repolarization

In accordance with the findings of Medina-Ravell[6], ECGSIM showed an increased transmural repolarization gradient directly under the LV pacing site during LV pacing. However, during RV pacing, TDR in the septum directly under the RV apical pacing site was also increased. This is not entirely unexpected, because the endocardial RV lead is, like the epicardial LV lead, located outside the left ventricle.

Average TDR in the whole heart model was approximately the same during all pacing modes and slightly increased compared to normal activation (29, 26, 27 and 18 ms during RV, LV, BIV pacing and normal activation, respectively). This can be explained on the basis of the repolarization maps (Figure 3). During pacing (panels B-D), the depolarization sequence is followed by a similarly shaped repolarization pattern that spreads from the pacing site through the ventricles. With increasing distance from the pacing site, the epi- to endocardial activation order, which accentuates local TDR, is lost. For example, observe the depolarization wavefront at the basal surface of the left ventricle during LV pacing (panel C). Major part of the LV base is depolarized by a wavefront that progresses in a direction approximately parallel to the ventricular walls. Such a depolarization order does not introduce a large TDR, as it does not advance the depolarization time of the epicardium as compared to the endocardium. Both LV epicardial and RV endocardial pacing create such transventricular de- and repolarization patterns. These patterns are, apart from their opposite direction, not essentially different from another. Although BIV pacing is performed from two pacing sites, similar transventricular repolarization patterns are induced in the greater part of the ventricles (panel D). Hence, TDR is similar during all pacing modes. However, the efficiency of an intact conduction system with well-synchronized endo- to epicardial activation throughout the heart is not attained by any pacing mode. Therefore, TDR is moderately larger during all pacing modes than during sinus rhythm.

Tapex-end interval

The Tapex-end interval is a measure of TDR in the wedge preparation of the LV free wall[8]. The apex of the T wave emerges when the transmural voltage gradients are maximal; *i.e.*, when the epicardial action potentials have their steepest decline in

amplitude. This was elegantly shown by Antzelevitch and co-workers[8]. Recently, the Tapex-end interval was reported to be increased in ECGs of heart failure patients during LV pacing. Based on the assumption that the laboratory situation (wedge) and the clinical situation (whole heart) are analogous, it was concluded that LV pacing increased TDR[6].

Our simulations suggest that other factors determine the Tapex-end interval during pacing of a whole heart. The occurrence of the apex of the T vector can be understood from the repolarization maps in Figure 3. During RV pacing (panel B) the repolarization wavefront increases in size when progressing from apex to base. The wavefront extends to its maximal area when it reaches the right ventricular base of the heart (t = 342 ms, green isochrone). At that moment the apex of the T vector emerges. During LV pacing (panel C), the repolarization wavefront has the largest area at 320 ms (green isochrone). However, at that moment repolarization has already progressed to the right ventricle before completion of the repolarization of the septum, which implies a certain amount of cancellation. This effect causes a relatively early occurrence (t = 300 ms, yellow isochrone) of the maximal T vector during LV pacing.
The end of the T vector occurs when the repolarization wavefronts have traveled to the most distant areas of the heart. In case of RV pacing the final repolarization occurs at the left ventricular base. In case of LV pacing the epicardium of the right ventricular free wall is the last area to repolarize. Final repolarization in both RV and LV pacing occurs in parts of the heart that are relatively distant from the area that generates the maximal repolarization vector. Therefore, neither the Tapex-end interval during RV pacing nor the Tapex-end interval during LV pacing express transmural dispersion of the repolarization. Thus, during pacing the Tapex-end interval contains information of the *global* transventricular repolarization process, whereas *local* repolarization differences in adjacent regions, like TDR, are considered more arrhythmogenic[27,28].

T-wave amplitude

Increase of T-wave amplitude has been related to increased dispersion of the repolarization by studies in biological and mathematical models. Increased TDR induced by hyperkalemia[29] or experimental Long QT 1 conditions[30] increases T-wave amplitude. Also, in ECGSIM experiments the T-wave amplitude increased with enhanced dispersion of the repolarization[13;25].

Hence, increased dispersion of the repolarization during regular, conduction-system mediated ventricular activation may cause high amplitude T waves. However, in the present study high amplitude T waves occurred during abnormal, cell-to-cell activation as a consequence of pacing. In the setting of pacing, TDR is relatively normal; the higher T-wave amplitude is here caused by less cancellation due to the asymmetric de- and repolarization sequence.

Of the different pacing modes, BIV pacing caused the lowest T-wave amplitude in our simulations and patients, as this pacing mode involves more cancellation due to the opposite directions of the two simultaneously started wavefronts (Figure 3D).

T-wave area

T-wave area has been related to dispersion of the repolarization in several studies. In rabbit hearts, dispersion of epicardial monophasic action potential duration was accompanied by increased T-wave area on a simultaneously recorded surface ECG[14]. In dogs, T-wave[31] and QRST[32] surface area were related to dispersion of repolarization and a lowered threshold for ventricular fibrillation[33]. We measured the smallest T-wave area during BIV pacing as compared to other pacing modes, in the patients as well as in our simulations. This low T-wave area during BIV pacing resulted from cancellation due to the opposite directions of the two simultaneously started wavefronts and was not due to an increased TDR.

T-wave complexity

Increased T-wave complexity in patients with arrhythmogenic right ventricular dysplasia has been associated with arrhythmias[34]. Long-QT patients can be distinguished from healthy subjects by an increased T-wave complexity[15]. In U.S. veterans with cardiovascular disease, repolarization complexity calculated with singular value decomposition conferred independent prognostic information[35]. Van Oosterom showed mathematically that T-wave complexity was related to dispersion of the repolarization induced by accentuated action potential duration differences[36]. In our study, the largest T-wave complexity was found during BIV pacing in heart failure patients and in the simulations. This is caused by the more complex repolarization pattern as a result of two colliding activation wavefronts instead of one. However, as stated earlier, the transventricular repolarization patterns and TDR are not essentially different from single-sided LV or RV pacing. Therefore, increased T-wave

complexity in BIV paced patients cannot be interpreted as an indication of increased arrhythmogeneity.

Limitations

Like every modelling study, the simulations with ECGSIM are a simplification of reality. The used model is not specifically designed as a heart failure model and lacks complex alterations in anatomy and electrophysiology present in varying degrees in heart failure patients. Recent mapping studies in heart failure patients during pacing and sinus rhythm have shown individually variable areas of slow conduction[37] and lines of functional block[38] resulting in complex depolarization patterns. However, also in these studies the largest areas were chiefly activated by slowly progressing wavefronts, suggesting myocardial cell-to-cell conduction, as we used in our simulations. We were able to simulate realistic ECGs in a model that has not been primarily designed for the current study. ECGSIM has been extensively evaluated and is sufficiently realistic to show the principles of repolarization and its effects on the ECG[13;39].

Conclusion

In patients treated with CRT, electrocardiographic repolarization indices are related to the pacing-induced activation sequences rather than to transmural dispersion. TDR during BIV and LV pacing is not larger than during conventional RV endocardial pacing.

REFERENCES

1. Abraham WT, Fisher WG, Smith AL, DeLurgio DB, Leon AR, Loh E, Kocovic DZ, Packer M, Clavell AL, Hayes DL, Ellestad M, Trupp RJ, Underwood J, Pickering F, Truex C, McAtee P, Messenger J: Cardiac resynchronization in chronic heart failure. N Engl J Med. 2002;346:1845-53.
2. John Sutton MG, Plappert T, Abraham WT, Smith AL, DeLurgio DB, Leon AR, Loh E, Kocovic DZ, Fisher WG, Ellestad M, Messenger J, Kruger K, Hilpisch KE, Hill MR: Effect of cardiac resynchronization therapy on left ventricular size and function in chronic heart failure. Circulation. 2003;107:1985-90.
3. Bradley DJ, Bradley EA, Baughman KL, Berger RD, Calkins H, Goodman SN, Kass DA, Powe NR: Cardiac resynchronization and death from progressive heart failure: a meta-analysis of randomized controlled trials. JAMA. 2003;289:730-40.
4. Cleland JGF, Daubert J, Erdmann E, Freemantle N, Gras D, Kappenberger L, Tavazzi L: The effect of cardiac resynchronization on morbidity and mortality in heart failure. New England Journal of Medicine. 2005;352:1539-49.
5. Fish JM, Di Diego JM, Nesterenko V, Antzelevitch C: Epicardial activation of left ventricular wall prolongs QT interval and transmural dispersion of repolarization: implications for biventricular pacing. Circulation. 2004;109:2136-42.
6. Medina-Ravell VA, Lankipalli RS, Yan GX, Antzelevitch C, Medina-Malpica NA, Medina-Malpica OA, Droogan C, Kowey PR: Effect of epicardial or biventricular pacing to prolong QT interval and increase transmural dispersion of repolarization: does resynchronization therapy pose a risk for patients predisposed to long QT or torsade de pointes? Circulation. 2003;107:740-6.
7. Yan GX, Lankipalli RS, Burke JF, Musco S, Kowey PR: Ventricular repolarization components on the electrocardiogram: cellular basis and clinical significance. J Am Coll Cardiol. 2003;42:401-9.
8. Yan GX, Antzelevitch C: Cellular basis for the normal T wave and the electrocardiographic manifestations of the long-QT syndrome. Circulation. 1998;98:1928-36.
9. Cowan JC, Hilton CJ, Griffiths CJ, Tansuphaswadikul S, Bourke JP, Murray A, Campbell RW: Sequence of epicardial repolarisation and configuration of the T wave. Br Heart J. 1988;60:424-33.
10. Franz MR, Bargheer K, Rafflenbeul W, Haverich A, Lichtlen PR: Monophasic action potential mapping in human subjects with normal electrocardiograms: direct evidence for the genesis of the T wave. Circulation. 1987;75:379-86.
11. van Oosterom A, Oostendorp TF: ECGSIM: an interactive tool for studying the genesis of QRST waveforms. Heart. 2004;90:165-8.
12. Moss AJ: Measurement of the QT interval and the risk associated with QTc interval prolongation: a review. Am J Cardiol. 1993;72:23-5.
13. van Oosterom A: Genesis of the T wave as based on an equivalent surface source model. J Electrocardiol. 2001;34:S217-27.
14. Zabel M, Portnoy S, Franz MR: Electrocardiographic indexes of dispersion of ventricular repolarization: an isolated heart validation study. J Am Coll Cardiol. 1995;25:746-52.
15. Priori SG, Mortara DW, Napolitano C, Diehl L, Paganini V, Cantu F, Cantu G,

Schwartz PJ: Evaluation of the spatial aspects of T-wave complexity in the long-QT syndrome. Circulation. 1997;96:3006-12.
16. Bazett HC: An analysis of the time relation of electrocardiograms. Heart. 1920;7:353-67.
17. Lay DC: Linear algebra and its applications. Second Edition. Reading, MA: Addison-Wesley, 2003, pp. 441-486.
18. Dower GE, Machado HB, Osborne JA: On deriving the electrocardiogram from vectoradiographic leads. Clin Cardiol. 1980;3:87-95.
19. Edenbrandt L, Pahlm O: Vectorcardiogram synthesized from a 12-lead ECG: superiority of the inverse Dower matrix. J Electrocardiol. 1988;21:361-7.
20. Faris OP, Evans FJ, Dick AJ, Raman VK, Ennis DB, Kass DA, McVeigh ER: Endocardial versus epicardial electrical synchrony during LV free-wall pacing. Am J Physiol Heart Circ Physiol. 2003;285:H1864-70.
21. Reddy VY, Neuzil P, Taborsky M, Kralovec S, Sediva L, Ruskin JN: Images in cardiovascular medicine. Electroanatomic mapping of cardiac resynchronization therapy. Circulation. 2003;107:2761-3.
22. Scher AM, Young AC: Spread of excitation during premature ventricular systoles. Circ Res. 1955;3:535-42.
23. Spach MS, Barr RC: Analysis of ventricular activation and repolarization from intramural and epicardial potential distributions for ectopic beats in the intact dog. Circ Res. 1975;37:830-43.
24. Vassallo JA, Cassidy DM, Miller JM, Buxton AE, Marchlinski FE, Josephson ME: Left ventricular endocardial activation during right ventricular pacing: effect of underlying heart disease. J Am Coll Cardiol. 1986;7:1228-33.
25. Hooft van Huysduynen B, Swenne CA, Draisma HH, Antoni ML, Van de Vooren H, Van der Wall EE, Schalij MJ: Validation of ECG indices of ventricular repolarization heterogeneity: a computer simulation study. J Cardiovasc Electrophysiol. 2005; 16: 1097-103
26. Wilson FN, MacLeod AG, Barker PS: The T deflection of the electrocardiogram. Trans Assoc Am Physicians. 1931;46:29-38.
27. Akar FG, Yan GX, Antzelevitch C, Rosenbaum DS: Unique topographical distribution of M cells underlies reentrant mechanism of torsade de pointes in the long-QT syndrome. Circulation. 2002;105:1247-1253.
28. El Sherif N, Caref EB, Chinushi M, Restivo M: Mechanism of arrhythmogenicity of the short-long cardiac sequence that precedes ventricular tachyarrhythmias in the long QT syndrome. J Am Coll Cardiol. 1999;33:1415-23.
29. Litovsky SH, Antzelevitch C: Transient outward current prominent in canine ventricular epicardium but not endocardium. Circ Res. 1988;62:116-26.
30. Shimizu W, Antzelevitch C: Cellular basis for the ECG features of the LQT1 form of the long-QT syndrome: effects of beta-adrenergic agonists and antagonists and sodium channel blockers on transmural dispersion of repolarization and torsade de pointes. Circulation. 1998;98:2314-22.
31. van Opstal JM, Verduyn SC, Winckels SK, Leerssen HM, Leunissen JD, Wellens HJ, Vos MA: The JT-area indicates dispersion of repolarization in dogs with atrioventricular block. J Interv Card Electrophysiol. 2002;6:113-20.
32. Abildskov JA, Green LS, Evans AK, Lux RL: The QRST deflection area of electrograms

during global alterations of ventricular repolarization. J Electrocardiol. 1982;15:103-7.
33. Kubota I, Lux RL, Burgess MJ, Abildskov JA: Relation of cardiac surface QRST distributions to ventricular fibrillation threshold in dogs. Circulation. 1988;78:171-7.
34. De Ambroggi L, Aime E, Ceriotti C, Rovida M, Negroni S: Mapping of ventricular repolarization potentials in patients with arrhythmogenic right ventricular dysplasia: principal component analysis of the ST-T waves. Circulation. 1997;96:4314-8.
35. Zabel M, Malik M, Hnatkova K, Papademetriou V, Pittaras A, Fletcher RD, Franz MR: Analysis of T-wave morphology from the 12-lead electrocardiogram for prediction of long-term prognosis in male US veterans. Circulation. 2002;105:1066-70.
36. van Oosterom A: Singular value decomposition of the T wave: its link with a biophysical model of repolarization. Int J Bioelectromagnetism. 2002;4:59-60.
37. Lambiase PD, Rinaldi A, Hauck J, Mobb M, Elliott D, Mohammad S, Gill JS, Bucknall CA: Non-contact left ventricular endocardial mapping in cardiac resynchronisation therapy. Heart. 2004;90:44-51.
38. Auricchio A, Fantoni C, Regoli F, Carbucicchio C, Goette A, Geller C, Kloss M, Klein H: Characterization of left ventricular activation in patients with heart failure and left bundle-branch block. Circulation. 2004;109:1133-9.
39. van Oosterom A: The dominant T wave and its significance. J Cardiovasc Electrophysiol. 2003;14:S180-7.